Antibacterial activity of biologically synthesized silver and zinc nanoparticles using *Allcemilla vulgaris* (Layd's mantle) leaf extract

Abstract

In this study, the powder of *Allcemilla vulgaris* was used in the sythesis of silver and zinc nanoparticle. Biologically synthesized nanoparticles were characterized using Scanning Electron Microscopy (SEM), Fourier transform infrared spectroscopy (FTIR), UV-Vis spectroscopy, X-ray diffraction (XRD) and Zeta potential and then evaluated for antibacterial potential using micro dilution broth method. The minimum inhibitory concentration values of AgNP were 4.25 µg/mL and 6.64 µg/ mL for *Escherichia coli* O157:H7 and *Staphylococcus aureus,* respectively. Similarly, the MIC values of ZnNP were 3.32 µg/mL and 6.25 µg/mL, respectively for *Escherichia coli* O157:H7 and *Staphylococcus aureus*.

Key words: Biological synthesis, silver, zinc, nanoparticle, *S.aureus*, *E.coli*, antibacterial activity

1. Introduction

Nanomaterials have got various applications in technology [1]. The metallic nanoparticles have large surface area so; they have antibacterial activity[2]. Nanoparticles can be synthesized by different physical, chemical and biological methods [3]. The risk of toxic compounds associated with chemical and physical methods limits the biomedical applications. So, the using of biological materials ie plants, plant components, bacteria for synthesis are safe and eco-friendly [4]. Plant based synthesis has some advantages for example it is faster and stable. It is possible to get different sizes and shapes of NPs comparable to microorganisms. Previous investigations showed silver and zinc nanoparticles to exhibit antibacterial, antioxidant and photocatalytic properties [5, 6]. Many studies showed that silver and zinc nanoparticles have

many good antimicrobial properties such as antibacterial, anti-viral, antifungal and anti-inflammatory activities as well as good stability [7, 8]. Due to these properties, silver and zinc nanoparticles have been used widely in the different industries such as in the health, food packaging, textile industries and other applications.

Alchemilla vulgaris is a perennial plant belonging to the Rosaceae family, which comprise of more than 300 species and commonly found in Africa, Asia, Europe, and the Americas. *A.vulgaris* benefits include treating muscle spasms, swelling and inflammation, digestive problems, water retention, mild diarrhea, and diabetes. This study aims at finding an easy and environmentally friendly use of silver and zinc nanoparticles using plant-based synthesis. Additionally, the evaluation of their antibacterial activity against *E.coli* and *S.aureus* which are known as human pathogenic bacteria was done.

2. Materials and methods

2.1. Bio-synthesis of silver and zinc nanoparticles

The methodological protocol by [9] was adopted with minor modifications. Briefly dried *A.vulgaris* plant (10 g) was added into 100 mL boiling deionized water for 30 min. The aqueous extract was left to cool at room temperature, and then filtered using Whatman No. 1 filter paper to a final volume of 80 mL. Ten (10) g of dried plant was added into 100 mL boiling deionized water for 30 min. The obtained extract was left to cool at room temperature, and then filtered using Whatman No. 1 filter paper. Final volume of plant extract was 80 mL. The filtrate was stored at 4 ^{0}C until further use in the green synthesis of AgNP and ZnNP.

Ten (10) ml of *A.vulgaris* aqueous extract was taken from the stock solution and 3 mM of $AgNO_3$ (90 mL) was dissolved in the *A.vulgaris* extract solution using magnetic stirrer to a final volume of 100 mL. The solution was heated at 60–80 ^{0}C. The color change of the mixture from light brown to grey indicated completion of nanoparticle synthesis and this was val-

idated by measuring point absorbance peak using UV–Vis spectroscopy. Another 10 mL of *A.vulgaris* aqueous extract was taken from the stock solution and 2 g of zinc nitrate hexahydrate crystal were added. The solution was mixed with magnetic stirrer and then heated at 60–80 ^{0}C to a final volume of 100 mL. At the end, nanoparticle synthesis of the mixture was validated by measuring peak absorbance with UV–Vis spectroscopy.

2.2. Characterization of bio-synthesized silver and zinc nanoparticles

Characterization of AgNP and ZnNP was done using a dynamic light scattering (DLS), UV-Vis spectrometry, scanning electron microscopy (SEM) and Fourier transform infrared spectroscopy (FT-IR). Crystalline metallic silver and zinc were examined by X-ray diffractometer. A few drops of the concentrated AgNP and ZnNP solution were deposited on a carbon tape covered stub, and left overnight for drying. Then, the stub was coated with gold using a sputter coater to produce clear images from the SEM (ZEISS EVO LS10). The AgNP and ZnNP were well dispersed in water and the solution was used to determine the absorbance of the AgNP and ZnNP. The well dispersed AgNP and ZnNP solution was further used in measuring the effective diameter of the AgNP and ZnNP with a DLS. The formation of the AgNP and ZnNP and existence of the plant extract on the surface of the AgNP and ZnNP were both proven by FT-IR. For FT-IR analysis, the AgNP and ZnNP solution was centrifuged at 10.000 rpm for 15 min and the precipitated AgNP and ZnNP were allowed to dry at 60 ^{0}C and then measured using FT-IR spectroscopy.

2.3. Microorganisms and growth conditions

The methodological procedure by [10] was adopted. In this study, microorganisms (*E.coli* O157:H7 NCTC 12900, *S.aureus* ATCC 29213) were obtained from the culture collections of Department of Food Hygiene and Technologies, Faculty of Veterinary, Erciyes University, Kayseri, Turkey. Microorganisms were plated on blood agar (Oxoid, CM0271)

and incubated at 37 ^{0}C for 18-24 h. After incubation, 2–3 colonies of each organism taken from blood agar were inoculated to 5 mL Mueller Hinton broth (Oxoid, CM0405) and incubated overnight at 37 ^{0}C. The suspension adjusted to 0.5 McFarland turbidity (approximately 10^8 cfu ml^{-1} for bacteria).

2.4. Determination of Antibacterial activity with Micro dilution Broth Method

The method by [10] was followed with minor modifications. Briefly biologically synthesized silver and zinc nanoparticles were tested against Gram (-) *E.coli* O157:H7 (NCTC 12900) and Gram (+) *S.aureus* (ATCC 29213). To determine the antibacterial activity, the minimum inhibitory concentration (MICs) was calculated according to the well broth micro dilution method. The biologically synthesized silver and zinc nanoparticles were made in two-fold concentrations of 6 serial dilution in Muller-Hinton broth (Oxoid, CM0405) in a 96-well microtiter plates. Afterwards, 100 µL of freshly grown bacteria was standardized until a bacterial number of 1×10^8 cfu ml^{-1} in Muller-Hinton broth was reached, was added to each well and. The micro dilution test also comprised of positive control without plant extract and negative control lacking microorganisms under the same conditions. Plates were incubated aerobically at 37 ^{0}C for 24 h. Then, the inhibition of bacterial growth was recorded and interpreted as the MIC [10,11]. The antibacterial activities of the NPs were compared with commonly used antibiotics including ciprofloxacin and vancomycin as positive control. Tests were performed in duplicate. Data were expressed as means ± standard error (SE) for each treatment (n=2). P values of $r\leq0.05$ were considered to be significant.

3.Results and Discussion

3.1.Characterization of AgNP and ZnNP suspensions

The results of SEM images of Ag and Zn nanoparticles are shown in Figure 1 A and B. Figures show that the size of the AgNP is around 35 nm and the size of the ZnNP is around 40

nm. Small aggregations were observed in the SEM image. The small aggregations of the AgNP may increase the dynamic size. The ZnNP show two absorbance peaks at 253 nm and 351 nm, which correspond to the presence of the plant extract on the ZnNP surfaces and ZnNP, respectively.

Figure 1 A and B near to here

Nano-particulate silver showed a well-defined absorption peak in visible region at 253 and 355 nm (Figure 2A). The interaction of AgNP with aqueous extract of *A.vulgaris* validated the reduction of Ag^{+} ions to Ag^{0} by the reactive groups that may get in turn oxidized to other species. Similarly, nano-zinc showed a well absorption peak in visible region at 253 and 351 nm (Figure 2B). The UV–Vis spectroscopy is generally used in different studies to examine the size and shape of nanoparticles in aqueous suspension. Sastry et al., (1998) stated that the optical absorption spectrum of metal nanoparticles is dominated by surface plasmon resonance (SPR) [12].

Figure 2A and B near to here

The formation of the AgNP and ZnNP and the presence of the plant extract as capping agents on the AgNP and ZnNP surfaces were evaluated by FT-IR (Perkin Elmer Spectrum 400, Figure 3 A,B and C). Figure A shows organic content of *A.vulgaris* plant extract. According to results, the O-H of the alcohol ring stretching was clearly observed at ~ 3254 cm^{-1} and the stretching band at ~1311 cm^{-1} was related to the alkyl halide group and C–F. Additionally, the alkylene (-C≡C-) and alkene (C-H) stretching merged peaks appeared at ~2101 cm^{-1} and ~1629 cm^{-1}, respectively. The alkane and alkene C-H stretching merged peaks appeared at ~2917 cm^{-1} and ~1497 cm^{-1}, respectively. The N-H of the amide ring stretching was clearly

observed at ~1606 cm^{-1}, and the stretching band at ~1321 cm^{-1} was related to the alkyl halide group and C–F. The bending vibration at ~833 cm^{-1} was assigned to the C–H of the carboxylic group. The N-H of the amide ring stretching was clearly observed at ~ 3208 cm^{-1} (Figure 3C) and The O-H of the alcohol ring stretching was clearly observed at ~ 3378 cm^{-1}(Figure 3B). The functional groups from plant tissues can interact with different kind of metal salts and this process determine to nanoparticles formation [13]. In this study, FT-IR results recognized the water soluble plant metabolites such as polyphenols, flavonoids, and organic acids were possibly responsible for the bio-reduction of silver and zinc ions into AgNP and ZnONP.

Figure 3 A, B and C near to here

The crystalline nature and pattern of powdered AgNP and ZnNP were recorded by X-ray diffractometer (BRUKER AXS D8) at scan rate of 0.02°/s using Cu-kα1 radiation (1.5406 Å, 45 kV, 40 mA). The AgNP and ZnNP precipitate was dried at 80 ^{0}C before XRD analysis to remove all the moisture on AgNP and ZnNP surface. The dry AgNP and ZnNP were scanned under the range of scattering angle (2θ) between 10˚ to 70˚. Figure 4A showed that, the peaks around 38.5˚, 44.5˚ and 65˚ (in 2θ) are assigned to (111), (200) and (220) planes of face centered cubic silver nanoparticles using JCPDS card No.04-0783.

Figure 4B indicated that the peaks around on some weak diffraction peaks at 10.1˚ and 85˚ (in 2θ) are assigned to (001) and (104), respectively. The obtained peaks are suitable for hexagonal wurtzite structure of zinc (JCPDS Card no: 36–145). Similar results were reported by Chena et al. (2011) and Pung et al. (2012) [14,15].

Figure 4 A and B near to here

Zeta potential was taken as the mean value of different measurements. Zeta potential on the surface of AgNP and ZnNP was found to be −22.5 mV and – 22 mV, respectively. This stability and zeta potential were clues for an electrostatic mechanism due to adsorption of seconder metabolites. The obtained zeta potential value for the bio-synthesized AgNP and ZnNP prove that they are stable. Obtained results from this study are agreed with obtained by Kitler et al., (2010) [16].

Figure 5 A and B near to here

3.2 Antibacterial Assay of AgNP and ZnNP

The silver and zinc nanoparticles demonstrated strong antibacterial activity against both tested bacterial strains in the MIC assay (Table 1). However, AgNP broadly presented a faintly higher efficacy than ZnNP. In detail, the MIC values of ZnNP and AgNP detected as values of 6.25 µg/mL and 6.64 µg /mL against *S.aureus,* respectively. Results indicated that 4.25 µg /mL and 3.32 µg /mL concentrations were sufficient for killing of *E.coli* O157:H7 with AgNP and ZnNP, respectively. Figure 6 and 7 shows the effect of AgNP and ZnNP on the growth inhibition of *S.aureus* and *E.coli*.

Table near to here

Figure 6 A and B near to here

Similar to present study, Bhumi and Savithramma (2014) reported that the ZnONP had antimicrobial effect on *E. coli* and *S.aureus* [15]. Navale et al (2015) detected that the MIC value of ZnONP against *S.aureus* was 40 µg/mL [17]. According to study conducted by Emami-Karvani et al (2011), ZnO nanoparticles have antibacterial effect at the 10 µg/mL concentrations against *E.coli* [18]. Similar observations reported by Mostafa et al (2015) suggested that the MIC of AgNP against *S.aureus* and E.coli were 2.5 and 2 µg/mL, respectively [19]. How-

ever, Fayaz et al (2010) showed that AgNP were effective to Gram negative bacteria at 30–35 µg/mL versus were effective against Gram positive bacteria at 65–80 µg/mL concentrations [20]. Shameli et al (2012) recorded that AgNP were effective against *S.aureus* and *Salmonella typhi* at 20 µL of AgNP [21].

Figure 7 A and B near to here

Zhang et al(2007) showed that the sizes of zinc nanoparticles are important for antibacterial activity [22]. Results from this study indicated that the biologically synthesized ZnONP have improved antibacterial activity. According to literature, ZnONP show antibacterial effects on both Gram-positive and Gram-negative bacteria [23-25]. The efficient antibacterial activity of this nanoparticle is related to nanoparticle's surface area [24,26,27]. Safavo et al (2018) stated that the antibacterial activity of ZnO increased with reducing particle size [28]. In another study, Agnihotri et al (2014) reported the MIC value of AgNP at 30 µg/mL for strains of *E.coli* [29]. This value is approximately higher than the MIC determined in our study (4.25µg/mL). The difference could be related to the particle size. In a related report, Reddy et al (2014) the MIC of ZnONP was found at 40 µg/mL for *Klebsiella pneumonia* [30]. Therefore, it can be emphasized here that our green-synthesized nanoparticles displayed better antibacterial effect compared to that observed in other studies. However, Zarei et al., 2014 reported that the MIC values of AgNP varied between 3.12–6.25 µg/mL for *L.monocytogenes*, *E.coli* O157:H7 and *S.typhimurium* [31].

Our results are supported by the observations obtained by different author's [32, 33]. According to studies, the differences in bacteria's cell membrane structure can cause the different nanoparticle toxicity. Different studies showed that after contact with the bacterial membrane, nanoparticles generates high rate of reactive oxygen species leading to the death of bacteria.

This results from chemical interactions between hydrogen peroxide and membrane proteins [34].

4. Conclusions

Bio-synthesis of AgNPs and ZnNPs using plant extracts is a promising eco-friendly approach for their wide applications in various domains of science and thereby life. In this study, AgNPs and ZnNPs synthesized using *A.vulgaris* extract were tested for their antibacterial activities. AgNPs and ZnNPs formation was justified by simple visual detection of color change in solution and wavelength such as absorbance spectrum generated in visible region (253-355 nm for Ag and 253-351 for Zn). While the capping of certain compounds with functional groups on AgNPs and ZnNPs surface were determined by FTIR spectrum. XRD pattern indicated the formation of pure Wurtzite structure of ZnONP. The SEM images confirmed the formation of hexagonal particles and the average particle size of the nanoparticles was found to be 35 nm for Ag and 40 nm for Zn. The bio-synthesized AgNPs and ZnNPs have showed good antibacterial activity against pathogenic bacteria compared to the antimicrobials currently on market. The antibacterial assays revealed that ZnO Nps has effective growth inhibition activities against both gram negative and gram positive bacteria.

References

1. Albrecht MA, Evans CW, Raston CL. Green chemistry and the health implications of nanoparticles.Green Chem. 2006; 8 :417-432.

2. Khalil KA, Fouad H, Elsarnagawy T, Almajhdi FN. Preparation and characterization of electrospun PLGA/silver composite nanofibers for biomedical applications. Int J Electrochem Sci. 2013;8:3483–93.

3. Mahdavi S, Jalali M, Afkhami A. Heavy metals removal from aqueous solutions using TiO_2, MgO, and Al_2O_3nanoparticles. Chem Eng Commun. 2013; 200:448-470.

4. Arockiya F, Parthiban C, Ganesh-Kumar V, Anantharaman, P. Biosynthesis of antibacterial gold nanoparticles using brown alga, *Stoechospermum marginatum* (kützing). *Spectrochimica Acta Part A:* Molec Biomolec Spectros. 2012; 99:166-173.

5. Shriniwas P, Subhash KT. Antioxidant, antibacterial and cytotoxic potential of silver nanoparticles synthesized using terpenes rich extract of *Lantana camara* L. leaves. Biochem Biophys Reports. 2017;1076-81.

6. Logeswari P, Silambarasan S, Abraham J. Ecofriendly synthesis of silver nanoparticles from commercially available plant powders and their antibacterial properties Scien Iran. 2013; 20 (3):1049–1054.

7. Klaus-Joerger T, Joerger R, Olsson E, Granqvist C. Bacteria as workers in the living factory: metal accumulating bacteria and their potential for materials science. Trends Biotechnol. 2001;19:15–20.

8. Ahmed S, Ahmad M, Swami B, Ikram S. A review on plants extract mediated synthesis of silver nanoparticles for antimicrobial applications: A green expertise. J Adv Res. 2016;7:17–28.

9. Koca FD, Demirezen Yılmaz D, Duman F, Öçsoy I. Comparison of phytotoxic effects of biosynthesised copper oxide nanoparticle and ionic copper on *Elodea canadensis*. Chem Ecol. 2018;34:1-16.

10. Ertaş Onmaz N, Abay S, Karadal F, Hizlisoy H, Telli N, Al S. Occurence and antimicrobial resistance of *Staphylococcus aureus* and *Salmonella* spp. in retail fish samples in Turkey. Mar Pollut Bull. 2015;90:242-246.

11. Hammer KA, Carson CF, Riley TV. Susceptibility of transient and commensal skin flora to the essential oil of *Melaleuca alternifolia* (tea tree oil). Am J Infect Control. 1996;24:186 189.

12. Sastry M, Patil V, Sainkar SR. Electrostatically controlled diffusion of carboxylic acid derivatized silver colloidal particles in thermally evaporated fatty amine films. J Phys Chem B. 1998;102:1404–1410.

13. Ganesh Babu MM, Gunasekaran P. Production and structural characterization of crystalline silver nanoparticles from *Bacillus cereus* isolate. Colloids Surf B. 2009;74:191–195.

14. Chena C, Yu B, Liu P, Liu JF, Wang L. Investigation of Nano-Sized ZnO Particles Fabricated by Various Synthesis Routes. J Ceram Process Res. 2011; 12: 420–425.

15. Swee-Yong P, Wen-Pie L, Azizan A. Kinetic Study of Organic Dye Degradation Using ZnO Particles with Different Morphologies as a Photocatalyst. Int J Inorg Chem. 2012; 1–9.

16.Kittler S, Greulich C, Diendorf J, Koller M, Epple M. Toxicity of silver nanoparticles increases during storage because of slow dissolution under release of silver ions. Chem Mater. 2010;22:4548–4554.

17.Bhumi G, Ratna Raju Y, Savithramma N. Screening of zinc oxide nanoparticles for cell proliferation synthesized through *Adhatoda vasica* nees. Int J Drug Dev Res. 2014;6(2):97-104.

18. Navale GR, Thripuranthaka M, Lateand DJ, Shind SS. Antimicrobial Activity of ZnO Nanoparticles against Pathogenic Bacteria and Fungi. JSM Nanotechnol Nanomed. 2015; 3(1):1033.

19. Emami-Karvani Z, Chehrazi P. Antibacterial activity of ZnO nanoparticle on gram positive and gram-negative bacteria. Afr J Microbiol Res. 2015;5(12):1368-1373.

20. Mostafa AA, Sayed SRM, Solkamy EN, Khan M, Shaik MR, Al-Warthan A, Adil SY. Evaluation of Biological Activities of Chemically Synthesized Silver Nanoparticles. J Nanomater. 2015;1-7.

21. Fayaz AM, Balaji K, Girilal M, Yadav R, Kalaichelvan PT, Venketesan R. Biogenic synthesis of silver nanoparticles and their synergistic effect with antibiotics: a study against Gram-positive and Gram-negative bacteria. Nanomed Nanotechnol Biol Med. 2010;6:103-109.

22.Shameli K, Ahmad MB, Jazayeri SD, Shabanzadeh P, Sangpour P, Jahangirian H, Gharayebi Y. Investigation of antibacterial properties silver nanoparticles prepared via green method. Chem Cent J. 2012;6(1):73.

23. Zhang LL, Jiang YH, Ding YL, Povey M, York D. Investigation into the antibacterial behaviour of suspensions of ZnO nanoparticles (ZnO nanofluids). J Nanopart Res. 2007 ;9:479-489.

24. Li S, Canas Carrell JE, Irin F, Atore FO, Green MJ. Determination of multiwalled carbon nanotube bioaccumulation in earthworms measured by a microwave based detection technique. Sci Total Environ. 2013 ;9(13):445-446.

25. Vijayakumara S, Mahadevana S, Arulmozhia P, Sriramb S, Praseetha PK. Green synthesis of zinc oxide nanoparticles using Atalantia monophylla leaf extracts: Characterization and antimicrobial analysis. Mat Sci Semicon Proc**.** 2018; 82**(**1**):** 39-45

26. Khatamia M, Varmac RS, Zafarniad N, Yaghoobie H, Saranif M, Kumarg VG. Applications of green synthesized Ag, ZnO and Ag/ZnO nanoparticles for making clinical antimicrobial wound-healing bandages. Sustainable Chem Pharm. 2018; 10:9–15

27. Vijaya J, Jayaprakash N, Kombaiah K, Kaviyarasu K, Kennedy LJ, Jothi Ramalingam R, Al Lohedan HA, Ali M, Mohammed V, Maaza M. Bioreduction potentials of dried root of Zingiber officinale for a simple green synthesis of silver nanoparticles: Antibacterial studies.J Photochem Photobio Biol. 2017 ;169 :178–185.

28. Padmavathy N, Vijayaraghavan R. Enhanced bioactivity of ZnO nanoparticles—an antimicrobial study. Sci Technol Adv Mater. 2008; 9 :035004.

29. Safawo T, Sandeep BV, Pola S, Tadesse A. Synthesis and characterization of zinc oxide nanoparticles using tuber extract of anchote (*Coccinia abyssinica* (Lam.) Cong.) for antimicrobial and antioxidant activity assessment. Open Nano. 2018;3:56–63

30. Agnihotri S, Mukherji S, Mukherji S. Size-controlled silver nanoparticles synthesized over the range 5–100 nm using the same protocol and their antibacterial efficacy. RSC Adv. 2014; 4:3974–3983.

31. Reddy LS, Nisha MM, Joice M, Shilpa PN. Antimicrobial activity of zinc oxide (ZnO) nanoparticle against *Klebsiella pneumoniae*. Pharm Biol. 2014;52:1388–1397.

32. Zarei M, Jamnejad A, Khajehali E. Antibacterial effect of silver nanoparticles against four foodborne pathogens. Jundishapur J Microbiol. 2014;7:8720.

33.Zhang LL, Jiang YH, Ding YL, Daskalakis N, Jeuken L, Povey M, Neill AJO, York DW. Mechanistic investigation into antibacterial behavior of suspensions of ZnO nanoparticles against *E. coli*. J Nanopart Res. 2010 ;12 :1625-1636.

34. Premanathan M, Karthikeyan K, Jeyasubramanian K, Manivannan G. Selective toxicity of ZnO nanoparticles toward Gram-positive bacteria and cancer cells by apoptosis through lipid peroxidation. Nanomed Nanotechnol. 2011;7 (2):184-192.

35. Stoimenov PK, Klinger RL, Marchin GL, Klabunde KJ. Metal oxide nanoparticles as bactericidal agents. Langmuir. 2002;18 :6679-6686.

Table 1: Minimum inhibitory concentrations of bio-synthesized nano/silver and zinc oxide against *S.aureus* and *E.coli*. Values represent mean ± S.E. (n=2; p≤ 0.05)

	S. aureus	*E. coli*
	MIC Values (control antibiotics) (μg/ml)	
Vancomycin	≥16± 0.0001	Not effective
Ciprofloxacin	≥14± 0.0001	≥4± 0.0005
	MIC Values (nanoparticle/plant extract) (μg/ml)	
AgNP	6.64 ± 0.001	4.25± 0.001
ZnONP	6.25± 0.0004	3.32± 0.00008
A.vulgaris plant exctract	Not effective	Not effective

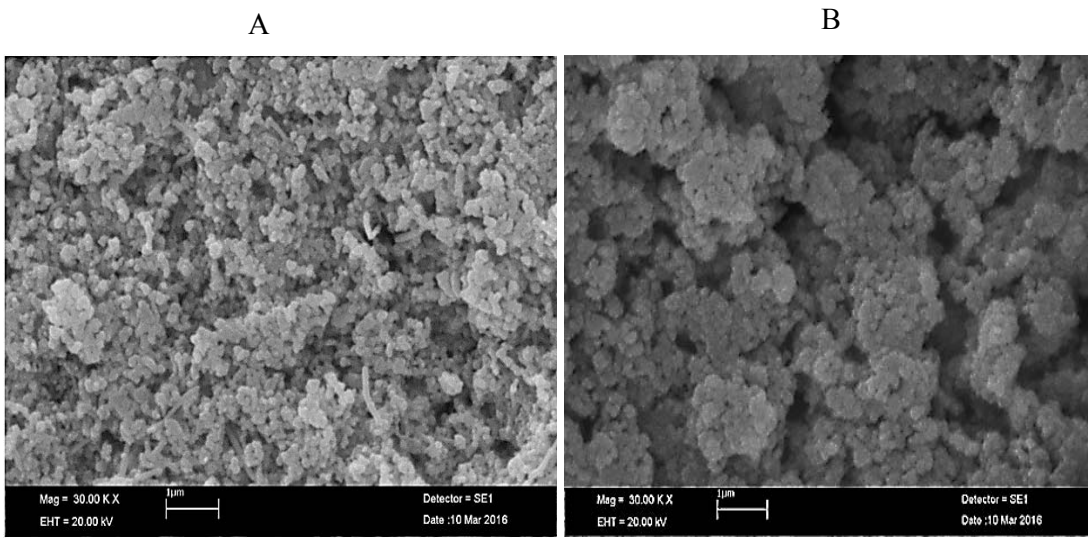

Figure 1: SEM image of silver nanoparticles (AgNP) (A) and zinc oxide nanoparticle (ZnONP) (B) in the *A.vulgaris* culture medium.

A

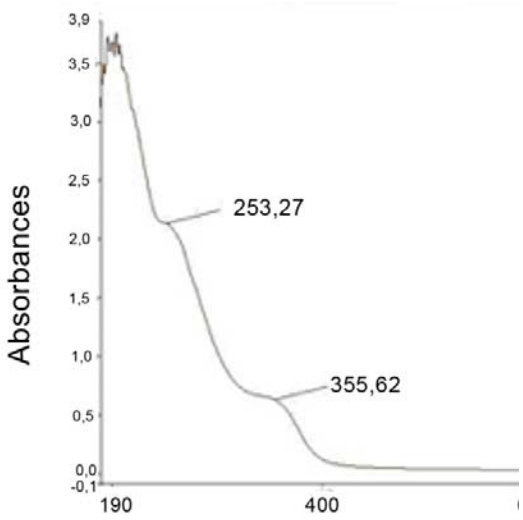

B

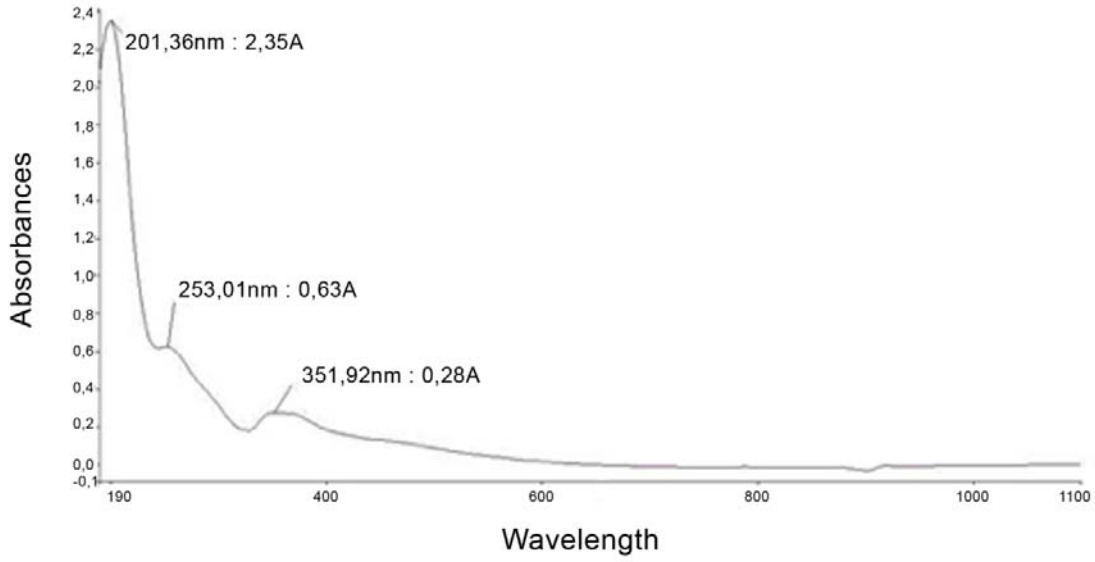

Figure 2: UV-Vis Spectra of silver nanoparticles (AgNP) (A) and zinc oxide nanoparticle (ZnONP) (B).

A

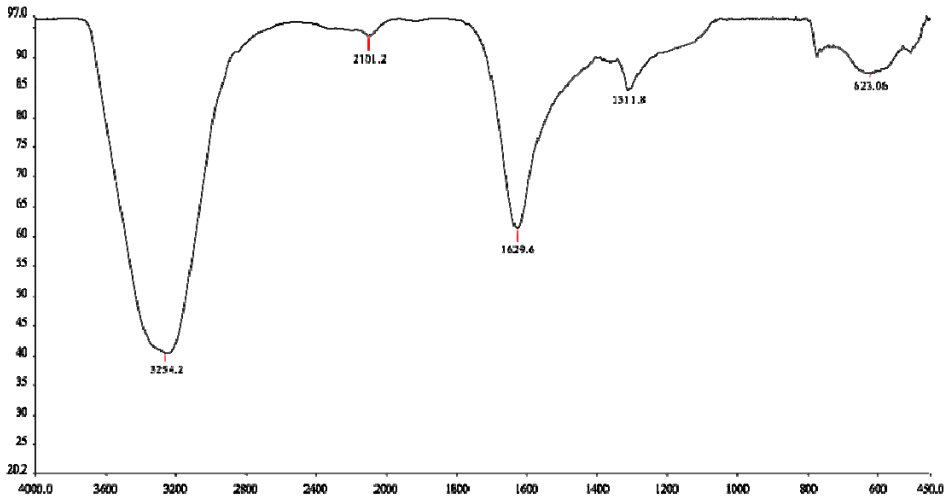
Transmittance %
97.0
90
85
80
75
70
65
60
55
50
45
40
35
30
25
20.2
3294.2
2101.2
1629.6
1311.8
623.06
4000.0
3600
3200
2800
2400
2000
1800
1600
1400
1200
1000
800
600
450.0
Wavenumbers (cm-1)

B

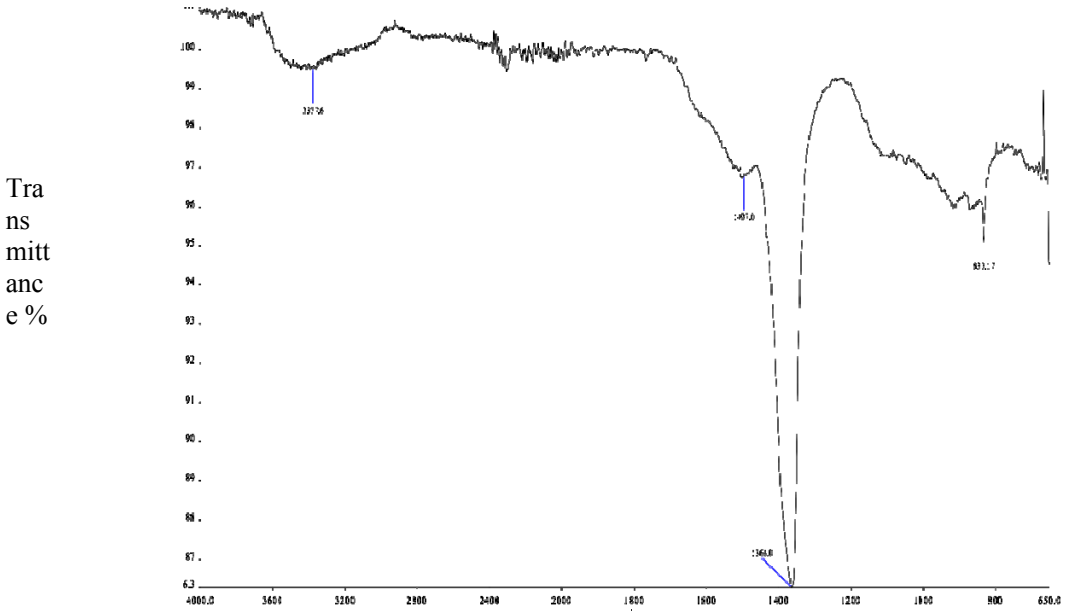
Transmittance %
100
99
98
97
96
95
94
93
92
91
90
89
88
87
6.3
3297.56
1407.0
1364.8
931.7
4000.0
3600
3200
2800
2400
2000
1800
1600
1400
1200
1000
800
650.0
Wavenumbers (cm-1)

C

Transmittance %

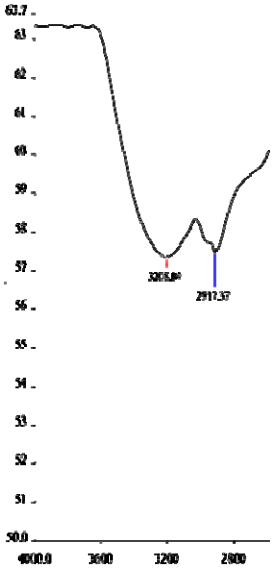

Wavenumbers (cm^{-1})

Figure 3: FTIR spectra of plant extract (A), silver nanoparticles (AgNP) (B), and zinc oxide nanoparticle (ZnONP) (C).

A

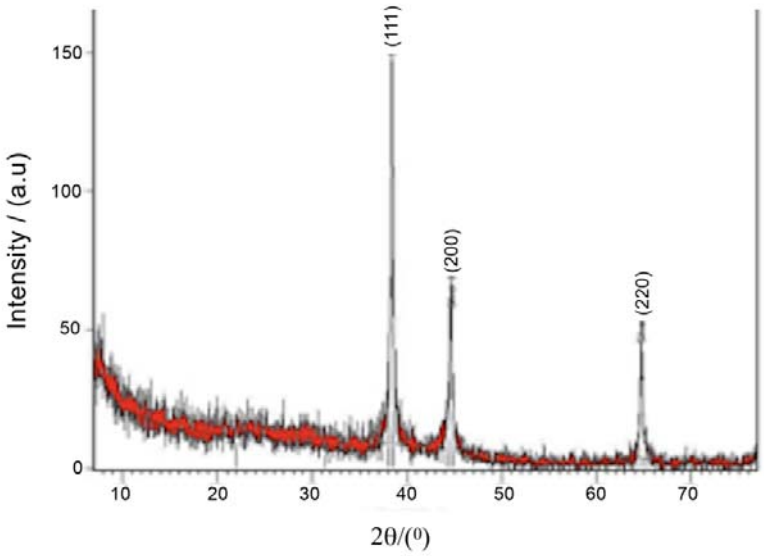

B

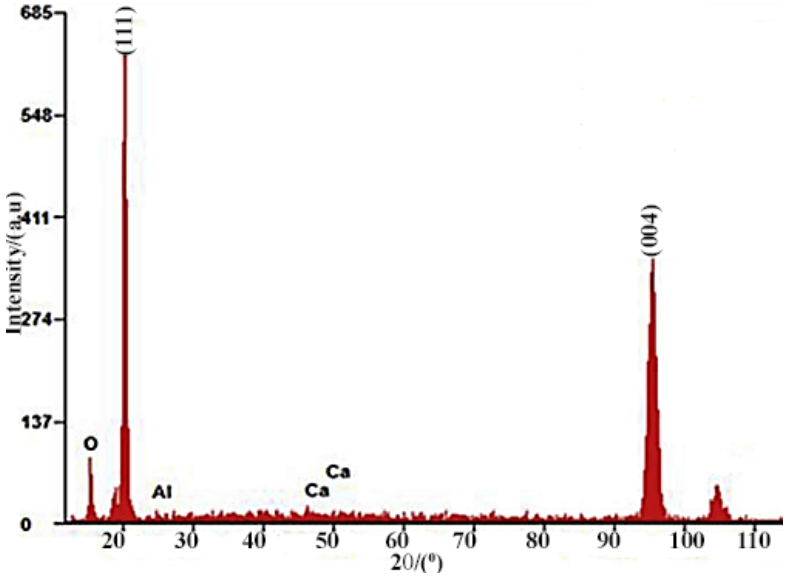

Figure 4: XRD patterns of AgNP (A) and ZnONP (B)

A

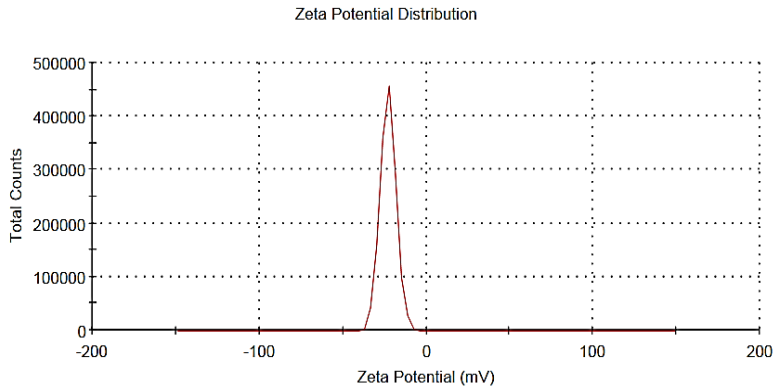

B

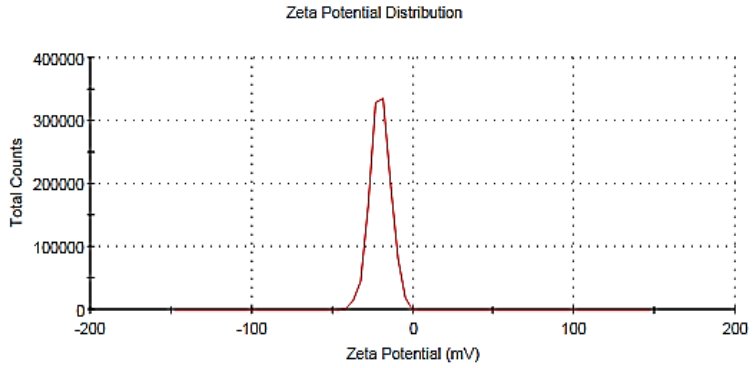

Figure 5: Zeta Potential Distribution for AgNPs (A) and ZnONPs (B)

A B

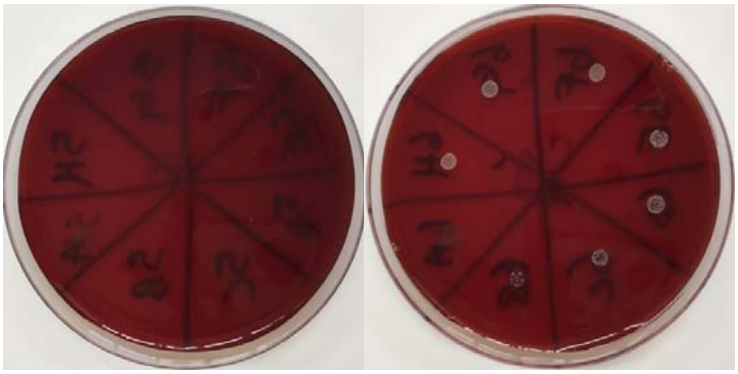

Figure 6: An image of inhibition zones for AgNP on *E.coli* (A) and *S.aureus* (B)

A B

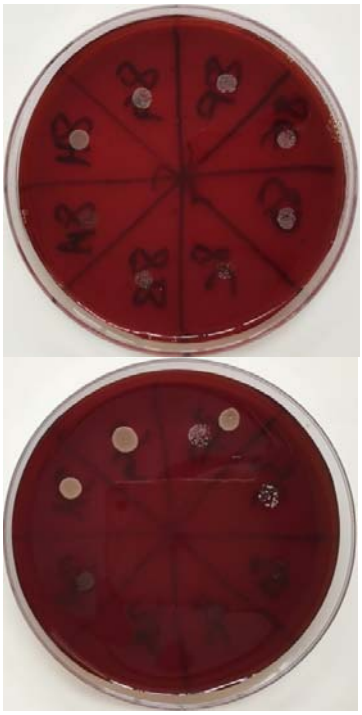

Figure 7: An image of inhibition zones for ZnONP on *E.coli* (A) and *S.aureus* (B)